

A JOINT RADAR-ACOUSTIC PARTICLE FILTER TRACKER WITH ACOUSTIC PROPAGATION DELAY COMPENSATION

Volkan Cevher, Milind Borkar, and James H. McClellan

Georgia Institute of Technology
Atlanta, GA 30332-0250

ABSTRACT

In this paper, a novel particle filter tracker is presented for target tracking using collocated radar and acoustic sensors. Real-time tracking of the target's position and velocity in Cartesian coordinates is performed using batches of range and direction-of-arrival estimates. For robustness, the filter aligns the radar and acoustic data streams to account for acoustic propagation delays. The filter proposal function uses a Gaussian approximation to the full tracking posterior for improved efficiency. To incorporate the aligned acoustic data into the tracker, a two-stage weighting strategy is proposed. Computer simulations are provided to demonstrate the effectiveness of the algorithm.

1. INTRODUCTION

Radar and acoustic measurements are complementary modalities for target tracking because their combination can determine a target's position in the Cartesian coordinates. In this paper, we present a particle filter for a radar-acoustic sensor that also adaptively synchronizes its multi-modal data streams for robust target tracking. Our focus is on collocated sensors, because the mapping of the range and bearing estimates into the target position estimate in 2D space is one-to-one.

The motivation for the joint acoustic-radar particle filter is the new low power RF sensor, implemented at the University of Florida, that transmits a microwave signal to determine the range, the velocity, and the size of detected targets [1]. The sensor is capable of providing range estimates at 32ms intervals with a range resolution of approximately 2m on a range-Doppler map. Up to 100m, the current system is capable of producing range estimates for multiple ground vehicles as well as human targets. The radar hardware is envisioned to have a larger detection range with hemispherical coverage in the future.

The particle filter is formulated using a state space approach. The state vector consists of the target position in Cartesian coordinates (x_t, y_t) and its velocity $(v_{x,t}, v_{y,t})$. We discuss the observability of this state vector given the particle filter multi-modal observations. The filter observations are based on batches of direction-of-arrival and range measurements. Hence, the received acoustic data and the radar pulse returns are first pre-processed to calculate the particle filter observations. These observations are adaptively synchronized by the particle filter to compensate for the acoustic propagation delays.

The filter state update function is based on a locally linear motion model. The filter observation equations are derived by using an image template matching idea. The template matching idea is very effective when accurate models are available [2]. In our problem, a temporal range image is first formed, when a batch of range measurements are received. Then, candidate image templates are formed by using the state update function and the target state vectors. By determining the best matching image template, the target state vectors are determined. It is assumed that the DOA and range

measurements are normally distributed around the true range measurements, with constant data miss-probability and clutter density.

To derive the particle filter proposal function, the target posterior density is approximately by Laplaces method: a Gaussian distribution around the posterior mode [3]. We calculate the posterior mode using a robust Newton-Raphson recursion with a backtracking step size selection that imposes smoothness constraints on the target motion [4–6]. Moreover, the particle filter incorporates an additional weighting stage because of the acoustic propagation delays. A *pre-weighting* stage re-weights the particle set representing the posterior from the previous iteration by using the lagged acoustic data received during the current estimation period.

2. TRACKER MECHANICS

In this paper, we focus the propagation delay aspect of the particle filter. The filter derivations assume that a single target is present.

The particle filter state vector $\mathbf{z}_t = [x_t, y_t, v_{x,t}, v_{y,t}]^T$ consists of the target position and velocity in Cartesian coordinates. The state vector is estimated at T second intervals (typically $T = 1$ s for ground targets) by using a batch of range and acoustic measurements (Fig. 1). It is assumed that the target moves with constant velocity during the estimation interval.

The received target multi-modal data is first processed by a proper beamformer and a radar processor at smaller intervals of $\tau = T/M$ (e.g., $M = 10$) to obtain a batch of target DOA and range estimates: $\mathbf{y}_{\theta,t} = \{\theta_{t+(m-1)\tau}(p_\theta)\}_{m=1}^M$ (acoustic) and $\mathbf{y}_{R,t} = \{R_{t+(m-1)\tau}(p_R)\}_{m=1}^M$ (radar), where m is the batch index, p_θ is the number of DOA estimates, and p_R is the number of range estimates per batch index (Fig. 2). It is assumed that the batch of measurements are normally distributed around the true target values with variances σ_θ^2 for acoustic DOA's and σ_R^2 for radar range measurements. The batch estimates may also include spurious peaks due to clutter that are Poisson distributed with rate λ_θ and λ_R for both modalities. In addition, a constant data miss probability q for each modality is assumed.

The observation data batches are treated as independent images using a template matching idea [2, 7, 8]. Figure 1 illustrates this idea for both modalities. Candidate image templates are formed by using the discrete realizations of the target state vector, called the *particles*. By determining how well each image template matches the observation image, a distribution for the particles is determined. Section 4 describes the equations that govern this process.

The particle filter adaptively synchronizes its multi-modal data to reduce estimation biases. Since electromagnetic waves and acoustic waves travel through the air at different velocities, range and DOA measurements received simultaneously do not represent information about the target's state at the same time. There is a time delay between the range and DOA measurements depending on the distance between the target and the sensors. This time-delay $t_d(t)$ can be calculated from the geometry of the system:

$$t_d(t) = \frac{1}{c} \sqrt{(x_t - s_x)^2 + (y_t - s_y)^2}, \quad (1)$$

where c is the speed of sound and (s_x, s_y) is the sensor position in Cartesian coordinates. Because of the target motion, there is also a

Prepared through collaborative participation in the Advanced Sensors Consortium sponsored by the U. S. Army Research Laboratory under the Collaborative Technology Alliance Program, Cooperative Agreement DAAD19-01-02-0008.

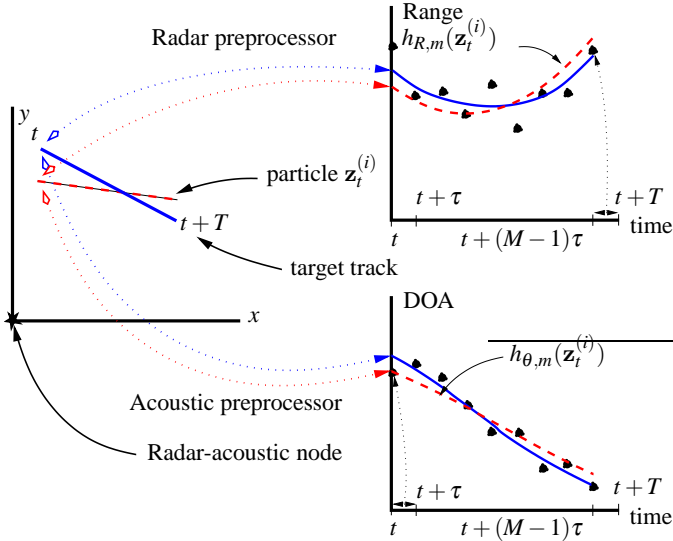


Figure 1: The radar range estimates and the acoustic DOA estimates are used to form temporal observation images. A candidate image template is formed by using a state vector realization (dashed line). The particle filter generates a distribution of these state vector realizations by determining how well each template matches the observation images.

doppler effect, similar to a time-warping operation, in the received acoustic data. The particle filter can handle this nonlinear doppler effect. However, for typical tracking scenarios involving ground targets, this effect is ignored in this paper and the time-delay is assumed constant during the estimation period T without loss of generality.

Figure 3 illustrates how the particle filter handles the received multi-modal data during an estimation period. The tracker performs estimation at the event time-frame for real-time tracking. Hence, the acoustic data received during the estimation period will correspond to actual events that occurred t_d seconds earlier. The filter uses the received radar range data (R_1, \dots, R_M) and part of the acoustic data $(\theta_{M_d+1}, \dots, \theta_M)$ to propose and weight its particles at the estimation period starting at time t . The remaining acoustic data $(\theta_1, \dots, \theta_{M_d})$ is used to pre-weight the particles that represent the posterior at $t - T$.

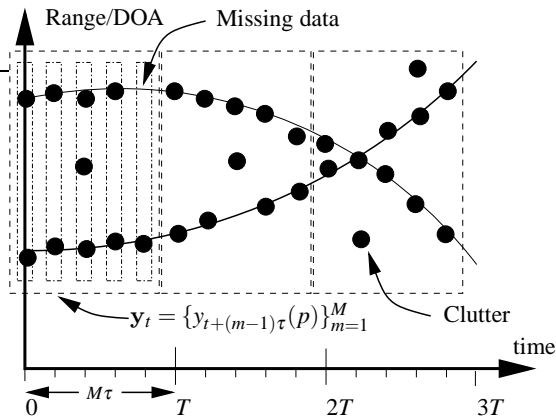


Figure 2: Observation data is not necessarily ordered. However, an image based observation approach provides a natural ordering, when targets are being tracked by the particle filter.

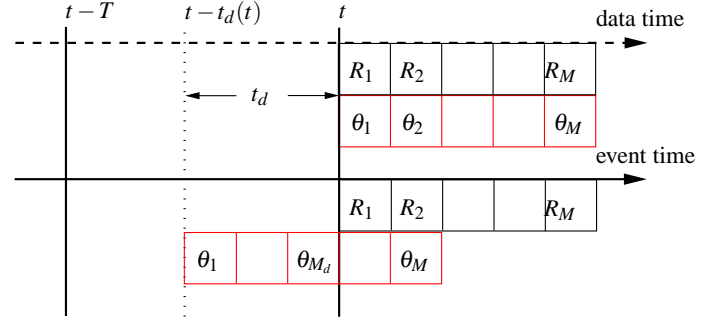


Figure 3: The received data time-frame does not coincide with the actual event time-frame due to the acoustic propagation delays. For real-time tracking, the received data must be properly aligned to reduce the estimation biases.

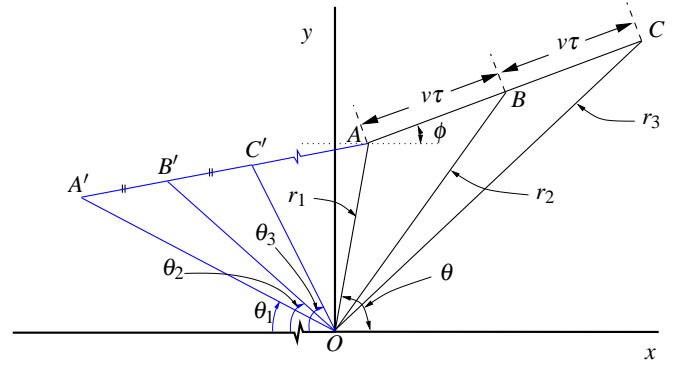


Figure 4: The target moves from A' at time $t - T$ to A in T seconds. The target speed during the batch starting at time t can be calculated as $v = \frac{1}{T} \sqrt{\frac{1}{2}(r_1^2 + r_3^2) - r_2^2}$. The DOA θ can be determined from the angle measurements $(\theta_1, \theta_2, \theta_3)$ by using the constant velocity assumption between $t - T$ and t .

3. OBSERVABILITY OF THE STATE VECTOR

Observability is a classical control theory concept that questions whether the state vector of a state-space system can be determined purely from its observations [9, 10]. In the joint radar acoustic tracking problem, it is intuitive that the state vector is observable when the radar batch data and the corresponding acoustic data overlap two or more batch observation measurements, resulting in two anchor space points from which the target velocity is also determined (i.e., $t_d \leq T - 2\tau$). In this section, we will give a stronger result and show that the state vector is observable even if there is no overlap, as long as $t_d \leq 2T - 3\tau$. This result also gives a bound on the maximum target tracking range ($R_{max} = (2T - 3\tau)c$) for real-time tracking.

Figure 4 illustrates that it is possible to determine the target speed v and the target heading minus the initial DOA $\phi - \theta$ given three range measurements [8]. This follows from Stewart's theorem that uses the law of cosines on the triangles $\triangle OAB$ and $\triangle OAC$. Note that the target DOA θ and the target heading ϕ can not be determined uniquely given only the range measurements. However, the DOA θ in Fig. 4 can be determined if three angle measurements are available from the previous batch. The proof uses the law of cosines on the triangles $\triangle OA'B'$ and $\triangle OA'C'$ and the constant velocity assumption [11, 12]. Therefore, if the current observed acoustic data allows us to observe three batch measurements that are within the previous estimation period time-frame, we can fully observe the current state.

4. DATA MODELS

4.1 State Update Density

The state update function can be derived from the physics of the target motion, which is modeled as locally linear. The resulting state update pdf is given by

$$p(\mathbf{z}_t | \mathbf{z}_{t-T}) = \mathcal{N}(\mathbf{A}_T \mathbf{z}_{t-T}, \Sigma_z), \quad (2)$$

where $\mathcal{N}(\mu, \Sigma)$ is the Gaussian density with mean μ and covariance Σ . The matrix \mathbf{A}_T comes from the linearization of the target motion:

$$\mathbf{A}_T = \begin{bmatrix} 1 & 0 & T & 0 \\ 0 & 1 & 0 & T \\ 0 & 0 & 1 & 0 \\ 0 & 0 & 0 & 1 \end{bmatrix}. \quad (3)$$

The noise covariance matrix Σ_z in (2) assumes a full rank diagonal form as opposed to the rank deficient form that models the correlations between position and velocity. In that case, the state update pdf includes Dirac's delta function and becomes unsuitable for the batch processing.

4.2 Observation Density

The particle filter observations $\mathbf{y}_t = [\mathbf{y}_{\theta,t}, \mathbf{y}_{R,t}]$ consist of the acoustic and radar observations that are assumed independent given the current state vector. Hence, the filter's multi-modal data-likelihood is a product of the individual likelihoods of each modality:

$$p(\mathbf{y}_t | \mathbf{z}_t) = p(\mathbf{y}_{\theta,t} | \mathbf{z}_t) p(\mathbf{y}_{R,t} | \mathbf{z}_t). \quad (4)$$

The radar returns and the received acoustic data over a time-interval τ are used to estimate target ranges and DOAs. A batch of M such range estimates are used by the particle filter to estimate the target state every $T = M\tau$ seconds. It is assumed that the batch of measurements are normally distributed around the true target ranges and a constant data miss probability q . The measurement batches may include spurious estimates due to clutter.

The observation density for each modality is derived using the arguments found in [13]. The clutter densities are given by

$$p(\theta | \theta \text{ is spurious}) = \lambda_\theta \text{ and } p(R | R \text{ is spurious}) = \lambda_R. \quad (5)$$

It is assumed that given the batch measurements, a single measurement from both modalities at each batch index m belongs to the target, or the target is missed for that modality. Multiple measurements imply the presence of clutter. Hence, the data likelihood is written as: $p(\mathbf{y}_t | \mathbf{z}_t) \propto$

$$\prod_{m=1}^M \left\{ 1 + \frac{1-q}{\sqrt{2\pi\sigma_R^2 q \lambda_R P_R}} \sum_{p_R=1}^{P_R} \exp\left(-\frac{(R_{t+(m-1)\tau}(p_R) - h_{R,m}(\mathbf{z}_t))^2}{2\sigma_R^2}\right) \right\} \\ \times \prod_{m=M_d+1}^M \left\{ 1 + \frac{1-q}{\sqrt{2\pi\sigma_\theta^2 q \lambda_\theta P_\theta}} \sum_{p_\theta=1}^{P_\theta} \exp\left(-\frac{(\theta_{t+(m-1)\tau}(p_\theta) - h_{\theta,m}(\mathbf{z}_t))^2}{2\sigma_\theta^2}\right) \right\}, \quad (6)$$

where t_d is calculated using (1) and quantized at levels of τ seconds, and the functions $h_{R,m}(\cdot)$ and $h_{\theta,m}(\cdot)$ (Fig. 1) are given by

$$h_{R,m}(\mathbf{z}_t) = \sqrt{(x_t + (m-1)\tau v_{x,t})^2 + (y_t + (m-1)\tau v_{y,t})^2}, \quad (7) \\ h_{\theta,m}(\mathbf{z}_t) = \tan^{-1}\left(\frac{y_t + (m-1)\tau v_{y,t}}{x_t + (m-1)\tau v_{x,t}}\right).$$

The approximation of t_d is not necessary if the particle filter tracker can give feedback to the acoustic beamformer that calculates the candidate DOA's. If feedback is possible, given the state vector \mathbf{z}_t , the acoustic data can be time-warped using (1), and the DOA's can be calculated accordingly. In this paper, because of the target ranges and the posterior variance, it happens that t_d is the same for most of the particles after quantization.

5. PARTICLE FILTER DETAILS

5.1 Proposal Function

Given the state-space description of a problem, the particle filtering solutions are well-understood. The efficiency of the algorithm depends on the proposal functions that determine the random support of the particles to be *properly* weighted for estimation. In this paper, a proposal function, denoted as $g(\mathbf{z}_t | \mathbf{y}_t, \mathbf{z}_{t-1})$, is derived to approximate the target posterior density directly:

$$g(\mathbf{z}_t | \mathbf{y}_t, \mathbf{z}_{t-1}) \approx p(\mathbf{z}_t | \mathbf{y}_t, \mathbf{z}_{t-1}) \propto p(\mathbf{y}_t | \mathbf{z}_t) p(\mathbf{z}_t | \mathbf{z}_{t-1}) \quad (8)$$

where $p(\mathbf{z}_t | \mathbf{z}_{t-1})$ is given by (2) and $p(\mathbf{y}_t | \mathbf{z}_t)$ is given by (6). Moreover, the proportionality in (8) is independent of the current state \mathbf{z}_t . This approximation, in effect, moves the particle stream towards high probability regions of the posterior, capturing the target maneuvers more effectively due to the reactive effect of the current observed data. Moreover, more particles survive the final resampling step, producing better future states as the system evolves [14].

The proposal function uses Laplace's method to approximate the data-likelihood term $p(\mathbf{y}_t | \mathbf{z}_t)$. Laplace's method is an analytical approximation of probability density functions based on a Gaussian approximation of the density around its mode, where the inverse Hessian of the logarithm of the density is used as a covariance approximation [15]. It can provide approximations to posteriors that are as accurate and sometimes more accurate than the approximations based on third-order expansions of the density functions [3]. This approach is also computationally attractive, because it only requires first and second-order derivatives. The condition for the accurate approximation is that the posterior be a unimodal density or be dominated by a single mode.

To calculate the mode of $p(\mathbf{y}_t | \mathbf{z}_t)$, denoted as \mathbf{z}_M , and the its Hessian \mathbf{H} at the mode, a Newton search algorithm with backtracking step size selection [4, 5] is used on the negative log-likelihood of (6). The algorithm is implemented based on the sufficient decrease condition. In this case, the Newton algorithm has numerical sensitivity issues. Hence, as an alternative, we change its cost function to the following cost function to determine the mode \mathbf{z}_M :

$$f_{\mathbf{z}}(\mathbf{z}_t) = f_\theta(\mathbf{z}_t) + f_R(\mathbf{z}_t) + f_{\hat{\mathbf{z}}}(\mathbf{z}_t), \quad (9)$$

where

$$f_\theta(\mathbf{z}_t) = \sum_{m=M_d+1}^M \sum_{p_\theta=1}^{P_\theta} \frac{(\theta_{t+(m-1)\tau}(p_\theta) - h_{\theta,m}(\mathbf{z}_t))^2}{2\sigma_\theta^2}, \quad (10)$$

$$f_R(\mathbf{z}_t) = \sum_{m=1}^M \sum_{p_R=1}^{P_R} \frac{(R_{t+(m-1)\tau}(p_R) - h_{R,m}(\mathbf{z}_t))^2}{2\sigma_R^2}, \quad (11)$$

and

$$f_{\hat{\mathbf{z}}}(\mathbf{z}_t) = \frac{1}{2}(\hat{\mathbf{z}} - \mathbf{z}_t)' \Sigma_e^{-1} (\hat{\mathbf{z}} - \mathbf{z}_t). \quad (12)$$

This cost function (9) is an approximation of the full posterior directly and consists of three terms: the first two terms have the same minima as the negative log-likelihood function of the data distribution; and the last term functions is a regularization term forcing the solution \mathbf{z}_M to lie close to some vector $\hat{\mathbf{z}}$ w.r.t. some weighted distance measure Σ_e . The parameter $\hat{\mathbf{z}}$ represents the particle best explaining the current data set, obtained by propagating forward the initial particle set coming from the previous time step by using the motion update.

Even with the available analytical relations, the calculation of the Hessian still poses problems. If the Hessian of (9) is directly calculated from the exact formulas, it is possible to show that the resulting expression for \mathbf{H} is not guaranteed to be positive definite and modifications are necessary to make the Newton correction effective at each iteration. Hence, while calculating the final expression of the Hessian, the terms including second-order derivatives

are neglected from the analytical formula. In this case, the Hessian is a function of the outer product of the gradient, and it is possible to prove that it is positive semi definite.

After the Gaussian approximation to the data-likelihood described above, the final expression for the proposal function to be used in the particle filter is given by

$$g(\mathbf{z}_t | \mathbf{y}_t, \mathbf{z}_{t-T}) \sim \mathcal{N}(\boldsymbol{\mu}_g, \boldsymbol{\Sigma}_g), \quad (13)$$

where

$$\begin{aligned} \boldsymbol{\Sigma}_g &= (\mathbf{H} + \boldsymbol{\Sigma}_z^{-1})^{-1}, \\ \boldsymbol{\mu} &= \boldsymbol{\Sigma}_g (\mathbf{H} \mathbf{z}_M + \boldsymbol{\Sigma}_z^{-1} \mathbf{A}_T \mathbf{z}_{t-T}). \end{aligned} \quad (14)$$

We note that at the proposal stage, any covariance approximation can be used because the particle filter's weighting stage can take care of any resulting discrepancies. Our particular covariance choice of the proposal function stems from the filter's efficiency concerns. Moreover, this proposal strategy also works even if there is no overlap between the acoustic and radar measurements, i.e., when $t_d \geq T$. This is because the last term in the cost function (9) keeps the cost function unimodal even if there is no acoustic information about the current target state. In this case, the inverse Hessian is not a good approximation for the data-likelihood covariance for the proposal and a constant preset covariance matrix can be used to propose particles.

5.2 Particle Weights

The weighting stage of the particle filter takes care of any discrepancies between how the particles are proposed and how the posterior is actually distributed. The particle filter algorithm for the joint particle filter has two weighting stages unlike the generic particle filter algorithm. The first weighting stage uses the subset of acoustic data ($\theta_1, \dots, \theta_{t_d}$ in Fig. 3) that carries information about the previous state. This stage is called the pre-weighting stage.

The pre-weights use the information in the current received acoustic data to reevaluate the importance of the particle set representing the posterior at time $t - T$. When there is no acoustic information about the current state (i.e., target range is more than Tc meters), the pre-weights may still allow the estimation of the state-vector (Fig. 5). Note that there is an state observability connection between Figs. 5 and 4. The pre-weights are given by the following expression based on the lagged data modality:

$$\begin{aligned} \hat{w}_t^{(i)} &= w_{t-T}^{(i)} p(\mathbf{z}_{t-T}^{(i)} | \mathbf{y}_t) \\ &\propto w_{t-T}^{(i)} p(\mathbf{y}_{\theta,t} | \mathbf{z}_{t-T}^{(i)}), \end{aligned} \quad (15)$$

where, by the Markovian property, $p(\mathbf{y}_{\theta,t} | \mathbf{z}_{t-T}^{(i)}) =$

$$\prod_{m=1}^{M_d} \left\{ 1 + \frac{1-q}{\sqrt{2\pi\sigma_\theta^2 q \lambda_\theta P_\theta}} \sum_{p_\theta=1}^{P_\theta} \exp \left(-\frac{(\theta_{t+(m-1)\tau}(p_\theta) - h_{\theta,m}(\mathbf{z}_{t-T}^{(i)}))^2}{2\sigma_\theta^2} \right) \right\}. \quad (16)$$

The particle filter weights for the current estimation time t are given by the ratio of the posterior density to the proposal density:

$$w_t^{(i)} = \hat{w}_t^{(i)} \frac{P(\mathbf{y}_t | \mathbf{z}_t^{(i)}) P(\mathbf{z}_t^{(i)} | \mathbf{z}_{t-T}^{(i)})}{g(\mathbf{z}_t^{(i)} | \mathbf{y}_t, \mathbf{z}_{t-T}^{(i)})}. \quad (17)$$

6. SIMULATIONS

Figure 6 shows the joint tracker with acoustic propagation delay compensation (solid line marked by \diamond) successfully tracking a maneuvering ground target (solid line). The target track begins at

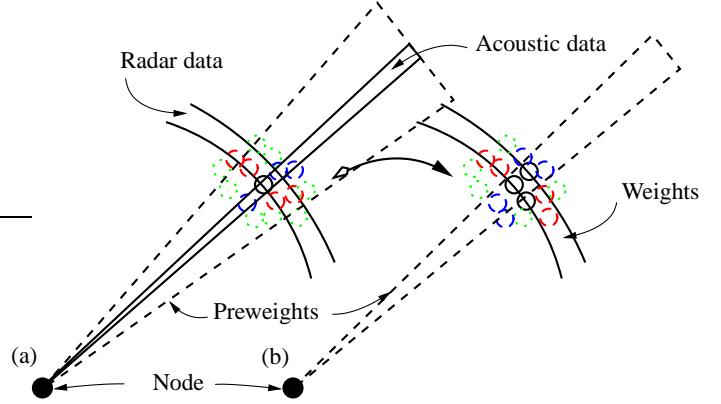


Figure 5: (a) When the acoustic and radar time-frames overlap, the final particle weights have contributions from (i) the radar-likelihood, (ii) the overlapping acoustic-likelihood, and (iii) the pre-weights (the residual acoustic-likelihood). (b) When there is no overlap between the radar and the acoustic data (i.e., $T \leq t_d \leq 2T - 3\tau$ in Fig. 3), the final particle weights still define a unimodal posterior through the contributions of the second stage weights and the preweights. Note that the distribution is tighter in (a) because there is more acoustic information available about the current state.

($-150\text{m}, 150\text{m}$). The target's speed in the x -direction is 15m/s , whereas the target's speed in the y -direction varies linearly from 25m/s to -25m/s . In the simulation, the radar-acoustic node is situated at the origin, and is assumed to have hemispherical coverage. Noisy measurements are simulated by adding independent zero mean white Gaussian noise with standard deviations of 1 degree and 2 meters to the DOA estimates and range estimates, respectively.

The top left plot in Fig. 6 also shows the biased tracking results without the time delay compensation (dashed line). The bias occurs because the filter tracks the delayed DOA observations (dashed line-top right plot in Fig. 6). The tracking bias increases with the target's velocity and also with the target's range from the radar-acoustic node. In this particular example, the acoustic DOA's are delayed more than one second between $t = 5\text{s}$ and $t = 15\text{s}$. However, because of the weighting strategy, the particle filter was able to track the target real-time.

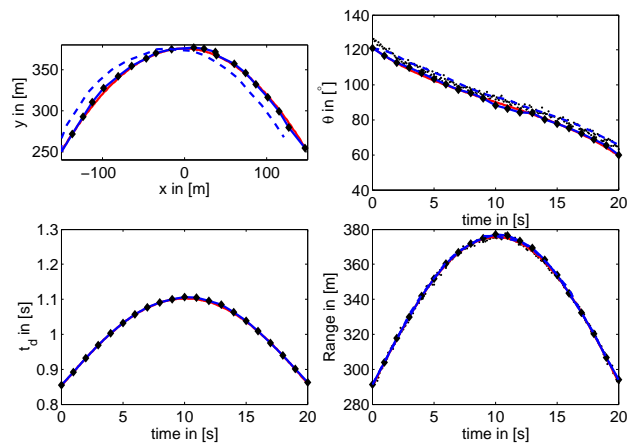


Figure 6: Tracking results with (solid line marked by \diamond) and without (dashed line) acoustic time-delay compensation are compared with the ground truth (solid line). The biased tracking results stem from the delayed acoustic data.

7. CONCLUSIONS

In this paper, we gave a particle filter solution to a joint acoustic radar tracking problem from a single node. Observability of the problem is discussed under real-time tracking constraints. A weighting strategy is proposed to tackle the acoustic propagation delays. The filter likelihood is formulated so that it is robust against missing data or spurious observations. We demonstrated the performance of the tracker in a real-time tracking scenario where the acoustic data is delayed about 1 second due to the target range. We showed that without the time-delay compensation, there is a bias in the state estimates due to rapid target motion.

REFERENCES

- [1] R. T. Damarla, V. Hao, C. Reiff, and J. Kurtz, "Fusion of acoustic and radar data for tracking vehicles," in *Military Sensing Symposium*, Laurel, MD, 22–25 August 2005.
- [2] M. Isard and A. Blake, *Active Contours*, Springer, 2000.
- [3] L. Tierney and J. B. Kadane, "Accurate approximations for posterior moments and marginal densities," *Journal of the American Statistical Association*, , no. 81, pp. 82–86, 1986.
- [4] J. Nocedal and S.J. Wright, *Numerical Optimization*, Springer-Verlag, 1999.
- [5] J.E.Dennis Jr. and R.B. Schnabel, *Numerical Methods for Unconstrained Optimization and Nonlinear Equations*, Society for Industrial and Applied Mathematics, Philadelphia, PA, 1996.
- [6] V. Cevher and J. H. McClellan, "An acoustic multiple target tracker," in *IEEE SSP 2005*, Bordeaux, FR, 17–20 July 2005.
- [7] V. Cevher and J. H. McClellan, "Acoustic direction-of-arrival multi target tracking," under revision at *IEEE Trans. on SP*.
- [8] V. Cevher, R. Velmurugan, and J. H. McClellan, "A range-only multiple target particle filter tracker," submitted to ICASSP 2006.
- [9] W.L. Brogan, *Modern Control Theory*, Prentice Hall, 1991.
- [10] T. Kailath, A.H. Sayed, and B. Hassibi, *Linear Estimation*, Prentice Hall, 2000.
- [11] Y. Zhou, P.C. Yip, and H. Leung, "Tracking the direction-of-arrival of multiple moving targets by passive arrays: Algorithm," *IEEE Trans. on Signal Processing*, vol. 47, no. 10, pp. 2655–2666, October 1999.
- [12] V. Cevher and J. H. McClellan, "General direction-of-arrival tracking with acoustic nodes," *IEEE Trans. on Signal Processing*, vol. 53, no. 1, pp. 1–12, January 2005.
- [13] Y. Bar-Shalom and T. Fortmann, *Tracking and Data Association*, Academic-Press, 1988.
- [14] J.S. Liu and R. Chen, "Sequential Monte Carlo methods for dynamic systems," *Journal of the American Statistical Association*, vol. 93, pp. 1032–1044, September 1998.
- [15] A. Gelman, J. B. Carlin, H. S. Stern, and D. B. Rubin, *Bayesian Data Analysis*, Chapman Hall/CRC, 2004.